Supramolecular Network Conducting the Formation of Uniaxially Oriented Molecular Crystal of Cyano Substituted Oligo(*p*-phenylene vinylene) and Its Amplified Spontaneous Emission (ASE) Behavior

Yupeng Li, Fangzhong Shen, Huan Wang, Feng He, Zengqi Xie, Houyu Zhang, Zhiming Wang, Linlin Liu, Feng Li,* Muddasir Hanif, Ling Ye, and Yuguang Ma*

State Key Laboratory of Supramolecular Structure and Materials, Jilin University, Changchun 130012, P.R. China

Received May 25, 2008. Revised Manuscript Received October 15, 2008

The supramolecular interactions are of importance for inducing the molecular orientation and constructing functional materials with high performance. In this manuscript we report uniaxially oriented molecular crystal of a cyano substituted oligo(*p*-phenylene vinylene) 1,4-bis(α-cyano-4-diphenylaminostyryl)-2,5-diphenylbenzene (CNDPASDB) with high luminescence under the driving force of the three-dimensional supramolecular interaction networks. Amplified spontaneous emission (ASE) with a low threshold value of 30.5 kW/cm^2 was observed from a high-quality slab-like CNDPASDB crystal and verified by the variable pump stripe method. The net gain coefficient with 55 cm^{-1} is also measured. The tip of CNDPASDB crystal exhibits polarized self-waveguided emission due to the propagation of polarized light emitted from the uniaxially oriented CNDPASDB molecules along crystal surface.

Introduction

Luminescent organic molecules and polymers have been widely investigated for light-emitting diodes (LEDs). An extended application of these luminescent materials is the solid-state laser, which has been the subject of numerous investigations. The phenomena of laser or amplified spontaneous emission (ASE) have been reported in some material systems, such as conjugated polymers,[1−4] dye doped systems,[5,6] and organic crystals.[7−12] At present, organic lasers are limited in the style of optical pumping, and the organic diode laser (electrically pumped) keeps being an object to achieve. The main problems of organic materials for the diode laser are the low stability and inferior carrier mobility. In this context, organic single crystal materials may be promising candidates for organic laser diodes (LDs) because of the following advantages. The first is the high thermo-stability of crystal materials as compared with amorphous materials, which is a metastable phase in thermodynamics and tends to transition to a more stable phase at a relative low temperature (glass transition temperature, T_g). The second is the high carrier mobility of crystals attributed to the very low content of impurity and the highly ordered molecule arrangement, as compared with amorphous materials. For example, the mobility of pentacene in single crystal is achieved to the level of 10 cm^2 V^{-1} s^{-1}, five orders higher than that in amorphous films.[13,14] The third is excellent optical properties of crystals, such as low light propagation loss due to low light scattering and self-waveguide and reflecting mirror structure due to the presence of natural cleavage plane (crystal face) in crystals with regular shape, especially in slab-like crystals.

Generally, ASE takes place when the active films constitute waveguides.[3,15] Accordingly a laser crystal with slab-like shape and larger size is ideal, due to the requirement of waveguide structure. For an organic laser crystal, the molecular orientation in the crystal is also very important, because the light emission of organic materials is from the exciton located on single molecule, and properties of photons (such as polarization) emitted from each single molecule are dependent on the molecular orientation and the orientation of molecular transition dipoles. The molecules in a crystal with the same orientation, so-called uniaxially oriented molecular crystal, may be a basic particularity to realize the ASE with low energy threshold. In this case the emitted

* Coresponding authors. E-mail: lifeng01@jlu.edu.cn (F.L.); ygma@jlu.edu.cn.

(1) Tessler, N.; Denton, G. J.; Friend, R. H. *Nature* **1996**, *382*, 695.
(2) Hide, F.; Diaz-Garcia, M. A.; Schwartz, B. J.; Andersson, M. R.; Pei, Q.; Heeger, A. J. *Science* **1996**, *273*, 1833.
(3) Tessler, N. *Adv. Mater.* **1999**, *11*, 363.
(4) McGehee, M. D.; Heeger, A. J. *Adv. Mater.* **2000**, *12*, 1655.
(5) Nagawa, M.; Ichikawa, M.; Koyama, T.; Shirai, H.; Taniguchi, Y.; Hongo, A.; Tsuji, S.; Nakano, Y. *Appl. Phys. Lett.* **2000**, *77*, 2641.
(6) Berggren, M.; Dodabalapur, A.; Slusher, R. E. *Appl. Phys. Lett.* **1997**, *71*, 2230.
(7) Yanagi, H.; Ohara, T.; Morikawa, T. *Adv. Mater.* **2001**, *13*, 1452.
(8) Ichikawa, M.; Hibino, R.; Inoue, M.; Haritani, T.; Hotta, S.; Koyama, T.; Taniguchi, Y. *Adv. Mater.* **2003**, *15*, 213.
(9) Park, S.; Kwon, O.-H.; Kim, S.; Park, S.; Choi, M.-G.; Cha, M.; Park, S. Y.; Jang, D.-J. *J. Am. Chem. Soc.* **2005**, *127*, 10070.
(10) Xie, Z.; Yang, B.; Li, F.; Cheng, G.; Liu, L.; Yang, G.; Xu, H.; Ye, L.; Hanif, M.; Liu, S.; Ma, D.; Ma, Y. *J. Am. Chem. Soc.* **2005**, *127*, 14152.
(11) Ichikawa, M.; Nakamura, K.; Inoue, M.; Mishima, H.; Haritani, T.; Hibino, R.; Koyama, T.; Taniguchi, Y. *Appl. Phys. Lett.* **2005**, *87*, 221113.
(12) Xie, W.; Li, Y.; Li, F.; Shen, F.; Ma, Y. *Appl. Phys. Lett.* **2007**, *90*, 141110.
(13) Dimitrakopoulos, C. D.; Malenfant, P. R. L. *Adv. Mater.* **2002**, *14*, 99.
(14) Lee, J. Y.; Roth, S.; Park, Y. W. *Appl. Phys. Lett.* **2006**, *88*, 252106.
(15) Li, F.; Solomesch, O.; Mackie, P. R.; Cupertino, D.; Tessler, N. *J. Appl. Phys.* **2006**, *99*, 013101.

10.1021/cm801427s CCC: $40.75
Published on Web 11/14/2008

photons having the same stamps may be beneficial to their correlation coupling for the amplification of light emission. In past decade, the molecular arrangement of conjugated materials in solid state has attracted much attention and been widely studied. By our knowledge, many linear π-conjugated molecules often preserve herringbone or π-stack structures.[16,17] Few reports about the uniaxially oriented molecular crystals were found.[18] It is difficult to make linear conjugated molecules packing as designed structure in crystals, because of the multiplicate conformation of organic molecules and the ubiquitous nondirectional interactions in the solid state such as weak van der Waals forces. Previously, the uniaxially oriented films of linear conjugated molecules have been achieved by various techniques, such as stretching,[19] rubbing,[20] Langmuir−Blodgett technique,[21] friction transfer method,[22] deposition technique on special substrate,[23,24] and solution zone-casting methods.[25] However, it is difficult to obtain the defect-free single crystal with large size and high quality by these assistant orientation-inducing methods. Generally, the organic molecular alignment primarily depends on the inherent self-assembling of intermolecular interactions. The supramolecular interaction networks mediated by intermolecular interactions play a critical role in restricting the relative orientation of molecules and enforcing a self-assembling process to generate the molecular networks with specific architectural and functional behaviors. However, strong intermolecular interactions such as $\pi-\pi$ interaction often lead to photoluminescence (PL) quenching of most of conjugated molecules in the aggregated state,[26] which is disadvantageous to the ASE with low energy threshold in crystals. Recent works in our groups and others have demonstrated the strong supramolecular interactions could induce the tight packing of molecules and the high luminescence efficiency in crystals.[27−29] Here we report on the uniaxially oriented molecular crystal of a cyano substituted oligo(*p*-phenylene vinylene) 1,4-bis(α-cyano-4-diphenylaminostyryl)-2,5-diphenylbenzene (CNDPASDB, Figure 1). The three-dimensional supramolecular networks not only induce the high luminescence efficiency but also conduct the formation of high-quality slab-like crystal with the uniaxially oriented molecular packing. This crystal exhibits the strong polarized self-waveguided emission and the amplified spontaneous emission (ASE) with low threshold. The net gain coefficient is also measured.

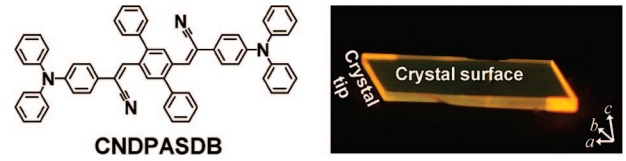

Figure 1. Structure of CNDPASDB and crystal photo under UV light.

Experimental Methods

Measurements. NMR spectra were recorded on a Bruker AVANCE 500 MHz spectrometer with chloroform-*d* as solvent and tetramethylsilane (TMS) as internal standard. The compound was characterized by a Flash EA 1112, CHNS-O elemental analysis instrument. Time-of-flight mass spectra were recorded using a Kratos MALDI-TOF mass system. IR spectra were recorded on a Perkin-Elmer spectrophotometer in the 4000−400 cm^{-1} region using a powdered sample dispersed in a KBr plate. The melting points were determined using a Germany NETZSCH (DSC-204) instrument differential scanning calorimeter at 10 °C/min with nitrogen flushing. Wide-angle X-ray diffraction was detected with a Rigaku X-ray diffractometer (D/max r A, using Cu Kα radiation of wavelength 1.542 Å).

Single Crystal X-ray Diffraction Data of CNDPASDB. The diffraction experiments were carried out on a Rigaku R-AXIS RAPID diffractometer equipped with a Mo Kα and Control Software using RAPID AUTO at 293 (±2) °C. The structures were solved with direct methods and refined with a full-matrix least-squares technique using the SHELXS v. 5.1 programs, respectively. The space groups were determined from the systematic absences, and their correctness was confirmed by successful solution and refinement of structures. Anisotropic thermal parameters were refined for all the non-hydrogen atoms. The positions of hydrogen atoms were located from difference maps and refined isotropically. CCDC 648738 contains the supplementary crystallographic data for this paper. These data can be obtained free of charge from the Cambridge Crystallographic Data Centre via www.ccdc.cam.ac.uk/data_request/cif or in the Supporting Information. Crystal data refinement conditions and experimental details are tabulated in Table 1.

Amplified Spontaneous Emission (ASE) Experiment. The slab-like crystal was optically pumped with Nd:YAG (yttrium−aluminum−garnet) laser (λ_{ex} = 355 nm, pulse duration 10 ns, repetition rate 10 Hz). The crystal size is about 1.5 mm × 1 mm × 5 μm. The energy of pumping laser was adjusted using calibrated neutral density filters. The beam was focused by using a cylindrical lens into a stripe whose shape was 4 × 0.5 mm^2 and was parallel to the long axis of this crystal which was glued on the quartz substrate. The emission from the tip of crystal was detected using a charge-coupled-device (CCD) fiber spectrograph. The polarization of light emitted from the tip of CNDPASDB crystal was measured by rotating a polarizer in front of the optical fiber.

Experimental Section

Synthesis of 2-(cyanomethyl)-4-(diphenylamino)benzene. To a solution of potassium tert-butoxide (4.6 mmol) in THF (10.2 mL) was slowly added under nitrogen atmosphere a solution of tosyl-

(16) Curtis, M. D.; Cao, J.; Kampf, J. W. *J. Am. Chem. Soc.* **2004**, *126*, 4318.
(17) Gierschner, J.; Ehni, M.; Egelhaaf, H.-J.; Medina, B. M.; Beljonne, D.; Benmansour, H.; Bazan, G. C. *J. Chem. Phys.* **2005**, *123*, 144914.
(18) Koren, A. B.; Curtis, M. D.; Francis, A. H.; Kampf, J. W. *J. Am. Chem. Soc.* **2003**, *125*, 5040.
(19) Weder, C.; Sarwa, C.; Montali, A.; Bastiaansen, C.; Smith, P. *Science* **1998**, *279*, 835.
(20) Jandke, M.; Strohriegl, P.; Gmeiner, J.; Brütting, W.; Schwoerer, M. *Adv. Mater.* **1999**, *11*, 1518.
(21) Cimrová, V.; Remmers, M.; Neher, D.; Wegner, G. *Adv. Mater.* **1996**, *8*, 146.
(22) Yoshida, Y.; Tanigaki, N.; Yase, K.; Hotta, S. *Adv. Mater.* **2000**, *12*, 1587.
(23) Yanagi, H.; Morikawa, T. *Appl. Phys. Lett.* **1999**, *75*, 187.
(24) Oehzelt, M.; Koller, G.; Ivanco, J.; Berkebile, S.; Haber, T.; Resel, R.; Netzer, F. P.; Ramsey, M. G. *Adv. Mater.* **2006**, *18*, 2466.
(25) Tracz, A.; Jeszka, J. K.; Watson, M. D.; Pisula, W.; Müllen, K.; Pakula, T. *J. Am. Chem. Soc.* **2003**, *125*, 1682.
(26) Cornil, J.; Beljonne, D.; Calbert, J.-P.; Brédas, J.-L. *Adv. Mater.* **2001**, *13*, 1053.
(27) Li, Y.; Li, F.; Zhang, H.; Xie, Z.; Xie, W.; Xu, H.; Li, B.; Shen, F.; Ye, L.; Hanif, M.; Ma, D.; Ma, Y. *Chem. Commun.* **2007**, 231.
(28) Xie, Z.; Yang, B.; Xie, W.; Liu, L.; Shen, F.; Wang, H.; Yang, X.; Wang, Z.; Li, Y.; Hanif, M.; Yang, G.; Ye, L.; Ma, Y. *J. Phys. Chem. B* **2006**, *110*, 20993.
(29) Dong, Y.; Lam, J. W. Y.; Qin, A.; Li, Z.; Sun, J.; Sung, H. H.-Y.; Williams, I. D.; Tang, B. Z. *Chem. Commun.* **2007**, 40.

Table 1. Crystal Data and Structure Refinement for CNDPASDB

identification code	CNDPASDB
empirical formula	$C_{60}H_{42}N_4$
formula weight	818.98
temperature (K)	293(2)
Wavelength (Å)	0.71073
crystal system	triclinic
space group	$P\bar{1}$
unit cell dimensions	
a (Å)	6.6429(13)
b (Å)	10.541(2)
c (Å)	16.573(3)
α (deg)	83.88(3)
β (deg)	86.20(3)
γ (deg)	84.05(3)
V (Å^3)	1145.9(4)
Z	1
D_{calcd} (mg/m^3)	1.187
absorption coefficient (mm^{-1})	0.069
F(000)	430
crystal size, mm	0.331 × 0.253 × 0.043
θ range for data collection	3.00−27.48 deg
reflections collected/unique	11257/5189 [R(int) = 0.0537]
completeness to θ = 27.48	98.4%
refinement method	full-matrix least-squares on F^2
data/restraints/parameters	5189/0/373
goodness-of-fit on F^2	1.018
final R indices [$I > 2\sigma(I)$]	R1 = 0.0644, wR2 = 0.1208
R indices (all data)	R1 = 0.1390, wR2 = 0.1505

methyl isocyanide (2.2 mmol) in anhydrous THF (3.4 mL). The resulting mixture was cooled at −40 °C, and a solution of 4-(diphenylamino)benzaldehyde (2 mmol) in anhydrous THF (3.4 mL) was slowly added. The mixture was stirred at −40 °C for 45 min followed by addition of MeOH (13.6 mL). The solution was heated at 80 °C for 20 min and cooled at room temperature. The solvent was removed under reduced pressure, and 2 mL of glacial acetic acid was added to the resulting dark solid. Water (40 mL) was added and washed three times with dichloromethane. The combined organic layer was dried over magnesium sulfate, and the solvent was removed under reduced pressure. The crude dark red viscous oil was purified by column chromatography (silica gel, 10% ethyl acetate in cyclohexane as eluent) to provide the brown solid in 50% yield. Mp 137−138 °C. ^{1}H NMR (500 MHz, 25 °C, $CDCl_3$, TMS, ppm): δ = 7.273−7.241 (t, 4H), 7.178−7.161 (d, 2H), 7.083−7.020 (m, 8H), 3.684 (s, 2H). FT-IR (KBr pellet, cm^{-1}): 3059, 3033, 2951, 2900, 2249, 1591, 1508, 1489, 1417, 1331, 1313, 1277, 1188, 1176, 1115, 1076, 843, 820, 800, 754, 696, 627, 611, 526, 509, 499.

Synthesis of 1,4-Bis(α-cyano-4-diphenylaminostyryl)-2,5-diphenylbenzene (CNDPASDB). [1,1′;4′,1″] Terphenyl-2′,5′-dicarbaldehyde (0.3 mmol) and 2-(cyanomethyl)-4-(diphenylamino)benzene (0.6 mmol) were dissolved in *tert*-butanol (2 mL) and THF (1 mL) at 50 °C under nitrogen atmosphere. Potassium *tert*-butoxide (0.05 mmol) and tetra-*n*-butylammonium hydroxide (0.05 mmol, 1 M solution in methanol) were added quickly, and the mixture was stirred vigorously at 50 °C. After 20 min the mixture was poured into acidified methanol. The precipitate was collected and dissolved in chloroform and then reprecipitated in methanol. The crude product was purified by column chromatography (silica gel, dichloromethane) under rigorous exclusion of light to give the yellow solid in 70% yield. Mp 306 °C (DSC). ^{1}H NMR (500 MHz, 25 °C, $CDCl_3$, TMS, ppm): δ = 8.233 (s, 2H), 7.530−7.470 (m, 8H), 7.433−7.393 (m, 8H), 7.298−7.267 (t, J = 8.240 Hz, 8H), 7.121−7.106 (d, J = 7.629 Hz, 8H), 7.094−7.064 (t, J = 7.324 Hz, 4H), 7.036−7.018 (d, J = 8.850 Hz, 4H). ^{13}C NMR (125 MHz, 25 °C, $CDCl_3$, TMS, ppm): δ = 149.011, 146.972, 141.402, 139.118, 138.601, 133.500, 130.376, 130.154, 129.500, 128.619, 128.125, 126.955, 125.232, 123.931, 122.171, 118.151, 113.244;

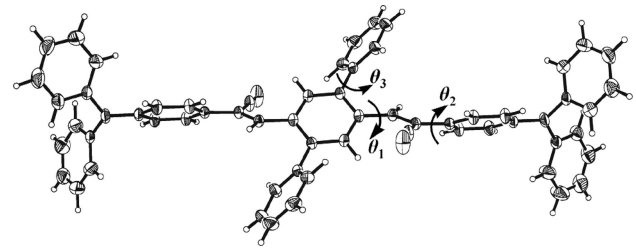

Figure 2. ORTEP structure of CNDPASDB.

FT-IR (KBr pellet, cm^{-1}): 3057, 3033, 2216, 1589, 1510, 1491, 1425, 1396, 1329, 1282, 1273, 1242, 1198, 1180, 1155, 1074, 1028, 912, 827, 754, 698, 617, 521, 474. Anal. Calcd for $C_{60}H_{42}N_4$: C, 87.99; H, 5.17; N, 6.84. Found: C, 87.26; H, 5.26; N, 7.01. MALDI-TOF MS: m/z = 819.9 ([M + H]$^+$); calcd for $C_{60}H_{42}N_4$, 818.98.

Results and Discussion

Synthesis and Characteristics. [1,1′;4′,1″] Terphenyl-2′,5′-dicarbaldehyde[30] and 4-(diphenylamino)benzaldehyde[31] were synthesized according to published procedures. 2-(Cyanomethyl)-4-(diphenylamino)benzene was prepared from 4-(diphenylamino)benzaldehyde upon treatment with tosylmethylisocyanide (TosMIC) and *t*-BuOK in one single step[32] with 50% yield. CNDPASDB was synthesized by a typical Knoevenagel condensation from 2-(cyanomethyl)-4-(diphenylamino)benzene and [1,1′;4′,1″] terphenyl-2′,5′-dicarbaldehyde in dry tetrahydrofuran (THF) solution catalyzed by potassium *tert*-butoxide (*t*-BuOK) and tetra-*n*-butylammonium hydroxide (TBAH). The crude product was precipitated from methanol and further purified by column chromatography under rigorous exclusion of light. The resulting compound CNDPASDB was obtained as yellow powder and fully characterized by NMR, FT-IR, elemental analysis, MALDI-TOF mass spectrum, and differential scanning calorimeter (DSC) methods.

Crystal Structure of CNDPASDB. The unit cell of CNDPASDB is triclinic, space group $P\bar{1}$, containing one discrete molecule. Crystal structure reveals that two double bonds of CNDPASDB molecule preserve *trans*-conformation. The molecule has a crystallographically imposed center of inversion, and the asymmetric unit contains one-half molecule. The ORTEP structure of CNDPASDB is shown in Figure 2. Similar to other 2PV with cyano substitute,[33] the CNDPASDB molecule in the crystal is remarkably twisted. The torsion angles between the double bond and two adjacent phenyl rings are 36° (θ_1) and 31° (θ_2), respectively. The torsion angle between the central phenyl ring and the adjacent phenyl ring (along the *p*-terphenyl direction) is 52° (θ_3), which is larger than that in *p*-terphenyl (38.4°). The generally twisted structure is unfavorable to the highly ordered alignment of molecules and the formation of high-quality crystal. But as shown in Figure 1, the transparent slab-like crystals with clear and sharp crystal faces of

(30) Xie, Z.; Yang, B.; Liu, L.; Li, M.; Lin, D.; Ma, Y.; Cheng, G.; Liu, S. *J. Phys. Org. Chem.* **2005**, *18*, 962.
(31) He, F.; Tian, L.; Tian, X.; Xu, H.; Wang, Y.; Xie, W.; Hanif, M.; Xia, J.; Shen, F.; Yang, B.; Li, F.; Ma, Y.; Yang, Y.; Shen, J. *Adv. Funct. Mater.* **2007**, *17*, 1551.
(32) Gómez, R.; Segura, J. L.; Martín, N. *J. Org. Chem.* **2000**, *65*, 7501.
(33) Oelkrug, D.; Tompert, A.; Gierschner, J.; Egelhaaf, H.-J.; Hanack, M.; Hohloch, M.; Steinhuber, E. *J. Phys. Chem. B* **1998**, *102*, 1902.

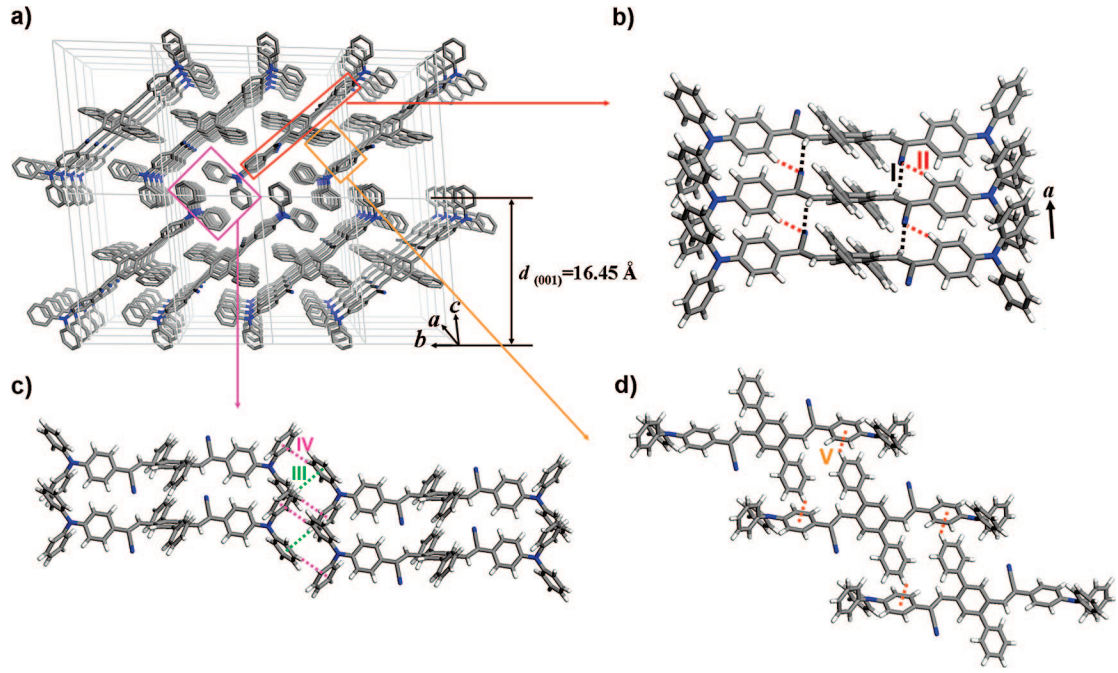

Figure 3. (a) Uniaxially oriented alignment of CNDPASDB molecules in the crystal. (b) C−H···N interactions I and II. (c) CH/π interactions III and IV. (d) CH/π interaction V.

CNDPASDB can be easily obtained, as vaporizing a solution of CNDPASDB in mixture of dichloromethane and methanol at room temperature under rigorous exclusion of light. Interestingly, all of the CNDPASDB molecules are found to array parallel with the identical conformation and orientation in the crystal and exhibit very regular uniaxially oriented packing (Figure 3a). According to meticulous analysis of the CNDPASDB crystal structure, we found it is the three-dimension supramolecular interaction networks that influence CNDPASDB molecules to assemble themselves into the absolute uniaxial orientation. As shown in Figure 3b, two types of short H−N distances exist between every cyano group on CNDPASDB molecules with two hydrogen atoms on double bond and phenyl of neighboring molecule and are shorter than the van der Waals distance of about 2.75 Å, indicating the presence of two types of C−H···N interactions I and II.[27,34−36] The H···N distances of two interactions I and II are 2.44(8) and 2.56(6) Å, and the C−H···N angles are 152° and 148°, respectively. Hence, the C−H···N interaction networks connect CNDPASDB molecules to construct the molecular clusters along *a* axial, in which each CNDPASDB molecule preserves the same orientation. Besides C−H···N interactions, there are three aromatic CH/π interactions (III, IV, and V) as shown in Figure 3c,d. The interaction distance and angle of C−H−π center for interaction III are 2.88(8) Å and 153°, for interaction IV are 2.87(2) Å and 156°, and for interaction V are 2.78(1) Å and 131°, respectively. The CH/π hydrogen bond (III and IV) networks attach the molecular clusters and conduct the uniform orientation of CNDPASDB molecules along the distyrylbenzene direction (Figure 3c). Moreover, CNDPASDB molecules have the CH/π hydrogen bonds (interaction V) and maintain the same orientation along terphenyl direction (Figure 3d).

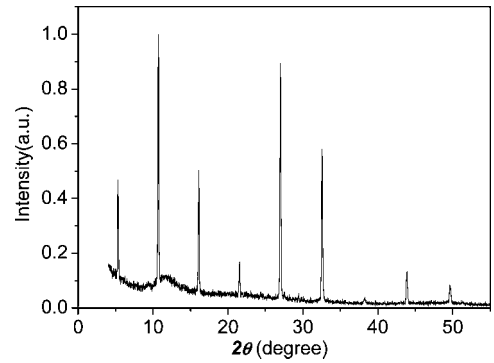

Figure 4. Wide-angle X-ray diffraction pattern of CNDPASDB crystal.

Figure 4 shows the wide-angle X-ray diffraction pattern of the slab-like CNDPASDB crystal. In the experiment, the suface of the slab-like crystal was parallel to the Si single crystal substrate. The strong diffraction peak at 5.32° corresponds to the diffraction spacing of ∼ 16.58 Å, and other equivalent periodic peaks at 10.7°, 16.1°, 21.54°, 27°, 32.54°, 38.26°, 43.86°, and 49.64° can be observed. The wide-angle X-ray diffraction (XRD) measurements of CNDPASDB crystal indicate that the diffractions comprise the primary diffraction spacing of ∼16.58 Å. Comparing the lattice constant with the XRD results, we notice that the primary diffraction spacing is approximately identical to $d_{(001)}$ (16.45 Å) of CNDPASDB crystal as shown in Figure 3a, which indicate that the *ab*-plane is parallel to the crystal surface of CNDPASDB (Figure 1).

Photophysical Properties of CNDPASDB. Figure 5 displays the UV−vis spectra in hexane, toluene, and tetrahydrofuran solution and the PL spectra in hexane, toluene,

(34) Taylor, R.; Kennard, O. *J. Am. Chem. Soc.* **1982**, *104*, 5063.
(35) T. Bartholomew, G. P.; Bazan, G. C.; Bu, X.; Lachicotte, R. J. *Chem. Mater.* **2000**, *12*, 1422.
(36) Yokoyama, T.; Yokoyama, S.; Kamikado, T.; Okuno, Y.; Mashiko, S. *Nature* **2001**, *413*, 619.

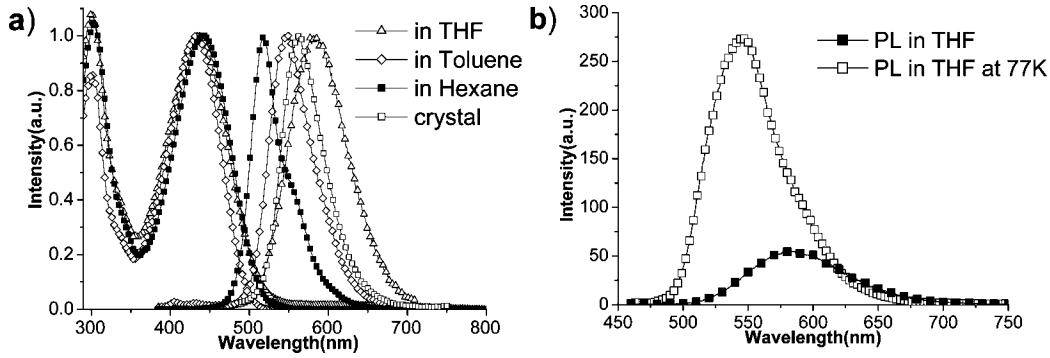

Figure 5. (a) UV−vis spectra and PL spectra normalized of CNDPASDB and (b) PL spectra of CNDPASDB at room temperature and 77 K in dilute THF solution (5×10^{-6} mol L^{-1}).

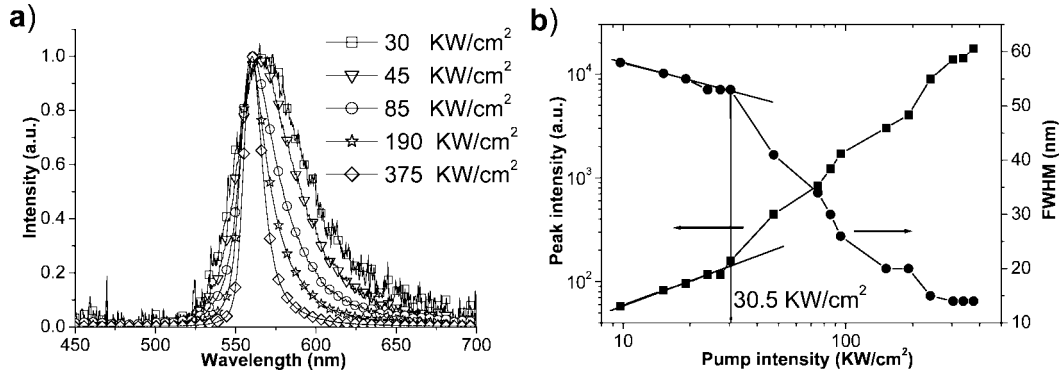

Figure 6. (a) PL spectra of CNDPASDB crystal as a function of the pump laser energy. (b) Dependence of the peak intensity and fwhm of emission spectra on the pump laser energy.

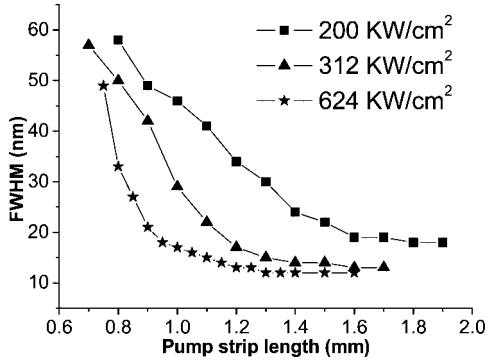

Figure 7. Dependence of the fwhm of PL spectra on the length of pump stripe at different pump energies.

and tetrahydrofuran solution and in crystal of CNDPASDB. The UV−vis spectra of CNDPASDB have two bands at 302 and 434 nm, showing very weak solvent dependence. The high-energy band about 302 nm is ascribed to the $\pi-\pi^*$ transition along the triphenyl axis, and the low-energy band about 434 nm is attributed to the $\pi-\pi^*$ transitions in backbone. The PL spectra of CNDPASDB exhibit strong dependence on solvent of different polarities (maximum PL peak at 519 nm in hexane, 549 nm in toluene and 583 nm in THF). This excited-state solvatochromism could result from the charge-transfer (CT) contributions between diphenylamine electron donor and electron-withdrawing cyano groups. The CNDPASDB crystal emits light of an orange color with $\lambda_{max,PL}$ at 562 nm.

The fluorescence yield of CNDPASDB is ∼9% in dilute THF solution. On the other hand, its crystals show enhanced emission with a fluorescence yield of ∼30% measured in a calibrated integrating sphere, which is similar to other twisted conjugated molecules with aggregation-induced emission (AIE).[27,28,37−39] In frozen glass state, such as the dilute THF solution (5×10^{-6} mol L^{-1}) at 77 K, CNDPASDB exhibits 4-fold enhancement of fluorescence and the PL intensity of CNDPASDB is higher than that at room temperature (Figure 5b). This property of CNDPASDB is similar to the CND-PDSB molecule without diphenylamino group and other twisted molecules with vinylene moiety because the easy nonradiating *cis−trans* photoisomerization of the vinylene moiety depresses the fluorescence in solution.[27,28,39−43] The easy photoisomerization can be clearly validated using the ^{1}H NMR spectrum by monitoring the CNDPASDB solution after exposure to daylight for several hours (see Supporting Information). The very rigid media at low temperature can enhance the potential barrier of free twisting motions of vinylene moiety and is beneficial to enhanced fluorescence. The fluorescence yield (∼30%) of CNDPASDB crystal is also approximately 4-fold higher than ∼9% in solution, which indicates that the strong supramolecular interaction

(37) Luo, J.; Xie, Z.; Lam, J. W. Y.; Cheng, L.; Chen, H.; Qiu, C.; Kwok, H. S.; Zhan, X.; Liu, Y.; Zhu, D.; Tang, B. Z. *Chem. Commun.* **2001**, 1740.
(38) An, B.-K.; Kwon, S.-K.; Jung, S.-D.; Park, S. Y. *J. Am. Chem. Soc.* **2002**, *124*, 14410.
(39) Bhongale, C. J.; Chang, C.-W.; Lee, C. S.; Diau, E. W.-G.; Hsu, C.-S. *J. Phys. Chem. B* **2005**, *109*, 13472.
(40) Sharafy, S.; Muszkat, K. A. *J. Am. Chem. Soc.* **1971**, *93*, 4119.
(41) Gruen, H.; Görner, H. *J. Phys. Chem.* **1989**, *93*, 7144.
(42) van Hutten, P. F.; Krasnikov, V. V.; Hadziioannou, G. *Acc. Chem. Res.* **1999**, *32*, 257.
(43) Li, Y.; Xu, H.; Wu, L.; He, F.; Shen, F.; Liu, L.; Yang, B.; Ma, Y. *J. Polym. Sci., Polym. Phys.* **2008**, *46*, 1105.

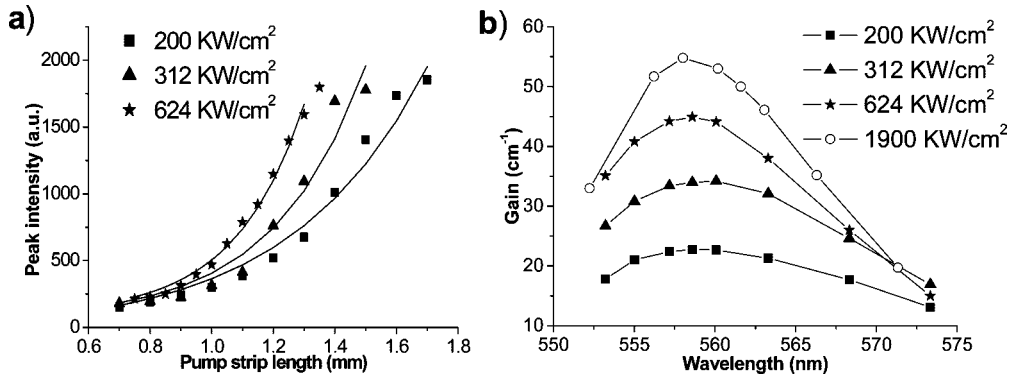

Figure 8. (a) Peak intensity of PL spectra as a function of the pump stripe length at different pump energies. (b) The net gain coefficient as a function of wavelength at different pump energies.

Table 2. Threshold of ASE for Different Organic Crystals

crystal no.	crystal growth method	threshold value (μJ/cm^{-2})	threshold value (kW/cm^{-2})	reference
CNDPASDB	solution	305 (10 ns)	30.5	this work
CNDPDSB	solution	395 (10 ns)	39.5	12
DPDSB	vapor	7000 (10 ns)	700	47
DPDSB	solution	13600 (10 ns)	1360	10
BP1T	vapor	27 (500 ps)	54	8
BP1T	solution	500 (500 ps)	1000	48
BP1T	melt-recrystallized	150 (500 ps)	300	49
BP2T	vapor	355 (500 ps)	710	8
BP3T	vapor	8 (500 ps)	16	11
BC4	vapor	50 (500 ps)	100	8
AC5	vapor	42 (500 ps)	84	8
P6T	vapor	750 (500 ps)	1500	50

networks similar to the rigid THF media at low temperature can well prevent the nonradiating intramolecular motions of CNDPASDB molecules in the crystal.

Amplified Spontaneous Emission of CNDPASDB Crystal. The tip of slab-like crystal shows stronger emission than the surface as shown in Figure 1, indicating the self-waveguided fluorescent emission of crystal. Generally, self-waveguided propagation of emission is thought to be one prerequisite for lasing or amplified spontaneous emission (ASE).[3,15] And the uniaxially oriented molecules should be a suitable configuration to amplify emitted light and achieve the organic crystal laser with low energy threshold because the light emission of organic materials is from excitons localized on a single molecule, and the dipole moments with the same configuration can easily interact into a certain phase with respect to the optical field, which should induce the coherent emission and the light amplification. The CNDPASDB crystal with size of 1.5 mm × 1 mm × 5 μm was optically pumped with a Nd:YAG (yttrium−aluminum−garnet) laser (λ_{max} = 355 nm, pulse duration 10 ns, repetition rate 10 Hz). The molar absorption coefficient of CNDPASDB molecule is 15 400 M^{-1} cm^{-1} at 355 nm, which indicates that the laser at 355 nm is a suitable light source to excite CNDPASDB molecules. When the pump energy increased, a gain-narrowed peak rises out of the broad emission spectrum (Figure 6a). Figure 6b represents dependence of the peak intensity and full widths at half-maximum (fwhm) of emission spectra on the pump laser energy. With the increase of pump energy, the FWHMs of emission spectra narrow from 58 nm at 9.7 kW/cm^2 to 14 nm at 304 kW/cm^2. The relationship between the peak intensity and the pump energy is nonlinear. This is characterized as the ASE caused by stimulated emission. The slope of peak intensity versus pump energy curve changes at 30.5 kW/cm^2, which should be the threshold value of ASE.

In succession the variable pump stripe method is used to verify the ASE and get the gain coefficient.[44,45] The length of pump stripe can be adjusted by a slit. As shown in Figure 7, the spectra are broad when the pump strip is short and become narrower with the increase of pump stripe length. The spectra narrowing at higher pump energy occurs more

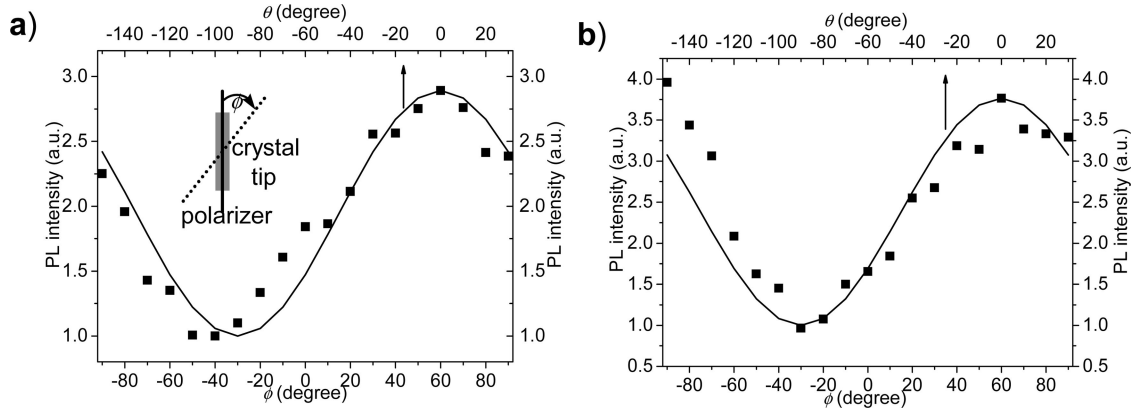

Figure 9. Dependence of the intensity (filled square) of polarized light from CNDPASDB crystal on the polarization angle ϕ at the energy of pumping laser about (a) 30 kW/cm^2 and (b) 1500 kW/cm^2. ϕ is the angle between the linear polarizer and the surface of slab-like CNDPASDB crystal. The solid curve is a fit to $\cos^2\theta$, ($\theta = \phi - 60°$, where θ is the angle between the polarization direction with the biggest intensity).

rapidly than that at lower pump energy as the pump stripe length increases. These facts are consistent with the prediction of ASE theory.

The peak intensity of PL spectra increases exponentially with the increase of pump stripe length as shown in Figure 8a. The solid curves are fits to the data using the following equation:

$$I(\lambda) = \frac{A(\lambda)P_0}{g(\lambda)}(e^{g(\lambda)l} - 1) \quad (1)$$

where A is a parameter proportional to the PL quantum yield, P_0 is the pump intensity, g is the net gain coefficient (subtract loss from gain), and l is the length of pump stripe.[44,45] By fitting the intensity data at different wavelengths of PL spectra, the curves of net gain coefficient versus wavelength can be obtained, as shown in Figure 8b. The peak of net gain is consistent with the peak of PL spectra, which indicates the stimulated emission is the strongest at the peak of PL spectra. The net gain coefficients at the peak can reach 55 cm^{-1} under the pump energy of 1900 kW/cm^2. This high value is comparable with those of the film materials such as bisfluorene-cored dendrimers and PFO.[46]

Table 2 summarizes the threshold values of ASE for most of organic crystals. The threshold value for the CNDPASDB crystal is among the lowest values, which is similar with the CNDPDSB crystal and extremely lower than the DPDSB crystals with cross stacking and staggered stacking, although CNDPASDB crystal exhibits low fluorescence yield (30%) compared with CNDPDSB and DPDSB crystals (80%).[10,27,47] And the threshold value for the CNDPASDB crystal is also approximate to the thiophene/phenylene co-oligomer crystals,[8,11] with herringbone packing[51,52] grown from vapor, and extremely lower than the thiophene/phenylene co-oligomer crystals grown from solution[48] and melt-recrystallized solid.[49] Compared with the BP1T crystal,[53] CNDPASDB crystal exhibits similar gain coefficient and an interestingly lower energy threshold of the ASE. The comparison indicates that the high-quality CNDPASDB crystal with regular uniaxially oriented molecules is suitable to amplify emitted light and achieve the laser with low threshold.

Polarized Emission of CNDPASDB Crystal. Normally, polarized emission is a direct consequence of the highly ordered alignment of π-conjugated molecules due to the intrinsic anisotropy of their electronic structure. The polarization of light emitted from the tip of the CNDPASDB crystal was measured at the energy of pumping laser about both 30 kW/cm^2 and 1500 kW/cm^2, as shown in Figure 9. The PL spectra from the tip of the CNDPASDB crystal at the energy about both 30 kW/cm^2 and 1500 kW/cm^2 show similar angle dependent polarization. The intensity of light polarized with an oblique angle $\sim 60°$ against the surface of slab-like CNDPASDB crystal is the biggest at the energy of pumping laser about both 30 kW/cm^2 and 1500 kW/cm^2. The least intensity of PL spectrum appear in the oblique angle $\sim -40°$ and $\sim -30°$ at the energy about 30 kW/cm^2 and 1500 kW/cm^2, respectively, which are approximatively perpendicular to the polarization direction with the biggest intensity. Calculated using ZINDO module of Cerius2 software, the orientation of the S0−S1 transition dipole moment of CNDPASDB against the molecular long axis is predicted to be $\sim 13°$ (see Supporting Information). According to crystal structure, the oblique angle of orientation of the transition dipole against the crystal surface (*ab*-plane) is $\sim 60°$, which is consistent to the direction with the biggest polarized intensity in the angular-resolved polarized fluorescence experiment. The angular-resolved polarized fluorescence intensities at both 30 kW/cm^2 and 1500 kW/cm^2 are curve-fitted using $\cos^2 \theta$, as shown in Figure 9, which is characteristic of the polarized emission from the uniaxially aligned chromophores[7,22,54] and indicates that the polarized tip emission of crystal is ascribed to the propagation of polarized light emitted from the molecules with uniaxial orientation along the crystal surface (*ab*-plane). However, the polarized ratios $I(\theta = 0°)/I(\theta = 90°)$ about 3.0 and 4.0 at the energies of about 30 kW/cm^2 and 1500 kW/cm^2 are lower than that of other linear conjugated molecules with uniaxial orientation,[19−23,54] which is probably due to the scattering of light emitted from CNDPASDB in the crystal and the high background emission at $\theta = 90°$.

Conclusion

We have demonstrated that directional supramolecular interaction networks enforce a self-organized uniaxial orientation of cyano substituted oligo(*p*-phenylene vinylene) CNDPASDB molecules. The supramolecular interactions have also a positive effect on the aggregation-induced emission (AIE) of CNDPASDB molecules by limiting the nonradiated process. The high-quality slab-like crystal of CNDPASDB reveals strong polarized self-waveguided emission. Amplified spontaneous emission (ASE) with low threshold value indicates that the CNDPASDB crystals with uniaxially oriented molecules are very suitable materials for the organic solid-state laser diodes.

Acknowledgment. We thank financial support from the National Science Foundation of China (Grants 50820145304, 20573040, and 50733002), the Ministry of Science and Technology of China (Grant 2002CB6134003), and PCSIRT. We thank Prof. Dongge Ma and Dr. Dingke Zhang for the help of the measurement of the fluorescence yield of crystals.

Supporting Information Available: ^{1}H NMR spectra, calculated transition dipole orientation (PDF), and an X-ray crystallographic file (CIF). This information is available free of charge via the Internet at http://pubs.acs.org.

CM801427S

(44) McGehee, M. D.; Gupta, R.; Veenstra, S.; Miller, E. K.; Díaz-García, M. A.; Heeger, A. J. *Phys. Rev. B* **1998**, *58*, 7035.
(45) Shaklee, K. L.; Leheny, R. F. *Appl. Phys. Lett.* **1971**, *18*, 475.
(46) Ribierre, J. C.; Tsiminis, G.; Richardson, S.; Turnbull, G. A.; Samuel, I. D. W.; Barcena, H. S.; Burn, P. L. *Appl. Phys. Lett.* **2007**, *91*, 081108.
(47) Xie, Z.; Wang, H.; Li, F.; Xie, W.; Liu, L.; Yang, B.; Ye, L.; Ma, Y. *Cryst. Growth Des.* **2007**, *7*, 2512.
(48) Nagawa, M.; Hibino, R.; Hotta, S.; Yanagi, H.; Ichikawa, M.; Koyama, T.; Taniguchi, Y. *Appl. Phys. Lett.* **2002**, *80*, 544.
(49) Hibino, R.; Nagawa, M.; Hotta, S.; Ichikawa, M.; Koyama, T.; Taniguchi, Y. *Adv. Mater.* **2002**, *14*, 119.
(50) Ichikawa, M.; Hibino, R.; Inoue, M.; Haritani, T.; Hotta, S.; Araki, K.; Koyama, T.; Taniguchi, Y. *Adv. Mater.* **2005**, *17*, 2073.
(51) Hotta, S.; Goto, M.; Azumi, R.; Inoue, M.; Ichikawa, M.; Taniguchi, Y. *Chem. Mater.* **2004**, *16*, 237.
(52) Hotta, S.; Goto, M. *Adv. Mater.* **2002**, *14*, 498.
(53) Bando, K.; Nakamura, T.; Masumoto, Y.; Sasaki, F.; Kobayashi, S.; Hotta, S. *J. Appl. Phys.* **2006**, *99*, 013518.
(54) Hagler, T. W.; Pakbaz, K.; Voss, K. F.; Heeger, A. J. *Phys. Rev. B* **1991**, *44*, 8652.